Available online at www.sciencedirect.com
SCIENCE DIRECT®
Journal of Power Sources 115 (2003) 153–160
JOURNAL OF POWER SOURCES
www.elsevier.com/locate/jpowsour

Studies of the performance of nanostructural multiphase nickel hydroxide

Xianyou Wang[a,b,*], Hean Luo[a], P.V. Parkhutik[b], Ari-Carman Millan[b], E. Matveeva[b]

[a]*College of Chemistry and Chemical Engineering, Xiangtan University, Hunan 411105, PR China*
[b]*Alcoy Higher School of Engineering, Universidad Politecnica de Valencia, Camino de Vera s/n, 46022 Valencia, Spain*

Received 27 June 2002; received in revised form 7 November 2002; accepted 28 November 2002

Abstract

The nanostructural multiphase nickel hydroxide, which was with doped at least three modifier elements has been synthesized. Scanning electron microscope (SEM) micrograph showed that the nanostructural multiphase nickel hydroxide was consisted of nanostructural particles. It has been confirmed by X-ray diffraction (XRD) examination that the compound has a mixed structure of α-$Ni(OH)_2$ and β-$Ni(OH)_2$. The tap-density of the nanostructural multiphase nickel hydroxide is 1.7–1.9 g/cm^3 and the discharge capacity can reach 375 mAh/g. The electrochemical studies revealed that the compound has much better redox reversibility, a much lower oxidation potential of Ni(II) than the corresponding oxidation state compared with β-$Ni(OH)_2$, and a much higher reduction potential. Since it has much higher tap-density and better electrochemical performance than Al-stabilized α-$Ni(OH)_2$ and usual β-$Ni(OH)_2$, it may be a promising positive active material for alkaline rechargeable batteries.

Keywords: Multiphase nickel hydroxide; Nanostructure; Cyclic voltrmmogram; Capacity

1. Introduction

Alkaline rechargeable batteries are most widely used in today's market covering domains of applications ranging from power tools to portable electronics and electric vehicle application. Nickel hydroxide was used as the active materials of the batteries, and the capacity of the batteries depend on one of the nickel hydroxide electrode. The development of nickel hydroxide have gone through from traditionally agglomerated nickel hydroxide to spherical β-$Ni(OH)_2$ [1]. Usually, electrode reaction of β-$Ni(OH)_2$ was considered to be a one-electron process involving oxidation of divalent nickel hydroxide to trivalent nickel oxyhydroxide on charge and subsequent discharge of trivalent nickel oxyhydroxide to divalent nickel hydroxide [2]. Thus, β-$Ni(OH)_2$ has a maximum theoretical specific capacity of 289 mAh/g. However, the development of today's electronic industry needs much higher energy density batteries, that is, a nickel hydroxide electrode which can provide for improved gravimetric energy density.

There are two polymorphs about the nickel hydroxide denoted by α-$Ni(OH)_2$ and β-$Ni(OH)_2$. Both forms crystallize in the hexagonal system with the brucite-type structure with $Ni(OH)_2$ layers stacked along the *c*-axis. Each $Ni(OH)_2$ layer consists of a hexagonal planar arrangement of octahedrally oxygen-coordinated Ni(II) ions. The main difference between the β- and α-type $Ni(OH)_2$ phase resides in the stacking of the layers along the *c*-axis. For the β-$Ni(OH)_2$ layers are perfectly stacked along the *c*-axis with an interlamellar distance of 4.6 Å; while for the α-$Ni(OH)_2$ layers are completely misoriented relative to each other corresponding to a turbostratic phase with the presence of water molecules and anionic species in the van der waals gap [3]. The interlamellar distance for the α-$Ni(OH)_2$ is about 7.5 Å [3].

It is found that α-$Ni(OH)_2$ has better electrochemical properties than β-$Ni(OH)_2$. The α-$Ni(OH)_2$ can be oxidized to γ-NiOOH in a lower potential than the corresponding oxidation state compared with β-$Ni(OH)_2$, and has a higher discharge capacity than β-$Ni(OH)_2$/β-NiOOH since the nickel oxidation in the γ-NiOOH is known to exceed 3, due to Ni^{4+} defects (3.3–3.7) [4]. Kamath et al. reported that a stabilized α-$Ni(OH)_2$ electrode has a much higher charge capacity than β-$Ni(OH)_2$ [5] and can be converted to γ-NiOOH reversibly without any mechanical deformation and swelling of the electrode during cycling process. However, α-$Ni(OH)_2$ is not stable in presence of the usual highly basic electrolyte media and transforms itself into β-$Ni(OH)_2$. Attempts to improve stability of the α-$Ni(OH)_2$

* Corresponding author. Fax: +86-732-231-9134.
E-mail address: xywang@xtu.edu.cn (X. Wang).

0378-7753/03/$ – see front matter © 2003 Elsevier Science B.V. All rights reserved.
doi:10.1016/S0378-7753(02)00649-3

have had a lot of reports [5–8]. Dixit et al. synthesized an aluminum-substituted α-$Ni(OH)_2$ by electrochemical impregnation and found it to deliver a reversible discharge capacity of ca. 450 mAh/g [6]. Faure et al. [7] studied pasted electrodes comprising cobalt-doped α-$Ni(OH)_2$ and found it had a capacity of 345 mAh/g. Ezhov and Malandin [8] found that zinc additive could stabilize the thermodynamically unstable α-$Ni(OH)_2$. Demourgues et al. reported that the chemical and physical properties of manganese-substituted nickel hydroxide with interlamellar water prepared by precipitation have been also reported [9,10]. Very recently Dai and Li [11] investigated that the structure, morphology and electrochemical performance of nanostructural aluminum-stabilized nickel hydroxides.

Although a lot of work have been carried out about α-$Ni(OH)_2$, and α-$Ni(OH)_2$ has much higher mass specific capacity than β-$Ni(OH)_2$, all α-$Ni(OH)_2$ synthesized have a low tap-density, and thus indicating a low volumetric specific capacity, therefore α-$Ni(OH)_2$ is never used in commercial batteries. The purpose of this paper is to synthesize a high density nanostructural multiphase nickel hydroxide, which was a mixed structure of α-$Ni(OH)_2$ and β-$Ni(OH)_2$. It exhibits both excellent electrochemical performance [12] and high tap-density; therefore it may be a promising positive active material for alkaline rechargeable batteries.

2. Experimental

All the reagents used were analytical reagent (AR) grade. The solution was prepared with water that was distilled and treated with a Millipore continental water system (Millipore Corporation). The nanostructural multiphase nickel hydroxide was synthesized by co-precipitation of several metal ions from the aqueous solution. The resulting brownish precipitate was filtered by a laboratory suction filter and washed with distilled water until it became a neutral salts, then dried at 80 °C. The doped metal ions are most preferably Co, Zn, and Mn.

Scanning electron microscope (SEM) measurements were carried out in the JSM6300 scanning microscope. The composition of the nanostructural multiphase nickel hydroxide and distribution of the elements in material was determined by EDX mapping which was attached by JSM6300 scanning microscope. The powder X-ray diffraction (XRD, PW1830, Philips Co.) with Cu Kα radiation was used to identify the phase. A study of the nanostructural multiphase nickel hydroxide was performed by infrared spectroscopy using a Perkin-Elmer Spectrum 2000 Fourier transform infrared (FTIR) spectrometer.

Measurement of the capacity of electrode was performed by filling active material to foam nickel substrate and conducting charge/discharge cycle, the capacity of 10th cycle was recorded as the capacity of the active material. The electrode substrate was prepared from 1 cm × 1 cm, thin sheets of nickel foam (porosity >95%). The multiphase nickel hydroxide was mixed with cobalt oxide powder at weight ratio of 7%, the appropriate amount of 1% polytetrafluorethylene (PTFE) aqueous suspension (60%) as a binder was added and kneaded to obtain paste. The paste was filled into the nickel foam substrate foam, after drying, the nickel foam plate was pressed into a thickness of 0.7 mm. Finally, the electrode was immersed in the electrolyte solution for 24 h.

Charge/discharge experiments were carried out using one nickel electrode coupling with two metal hydride (MH) electrodes. A separator film was used to prevent the electrodes from short circuit. Charge was initially carried out at a rate of 0.2*C* for 150% theoretical capacity, hold for 30 min., then discharge was performed at a rate of 0.2*C* to 0.1 V versus Hg/HgO.

Electrochemical measurements were performed using an EG&G PARC Model 273A Potentiostat/galvanostat and a typical three-electrode one-compartment electrolysis cell. The data were acquired with a personal computer. The working electrode is a powder microelectrode with diameter 200 μm platinum. Nickel sheet counter electrode was placed in the side and the working electrode was positioned in the center. A luggin capillary with a salt bridge was used to connect the cell to the reference electrode. All potentials were measured and quoted with respect to a Ag/AgCl (3 M NaCl) reference electrode.

3. Results and discussion

Fig. 1a shows the SEM micrograph of the nanostructural multiphase nickel hydroxides. In order to clearly show the characteristic of the particles, Fig. 1b is the SEM micrograph increased by further magnification. SEM examinations show that the samples are made up of monolithic particles and some of the particles agglomerated together to form a quasi-spherical shape. The single particles agglomerated in quasi-spherical shape through any physical or chemical process when they were synthesized. The tap-density measurements showed that it had a tap-density between 1.7–1.9 g/cm^3. The size of these particles distributed from some decade nanometer to some hundred nanometer. This explain the reasons that the tap-density of the nanostructural multiphase nickel

Table 1
The composition of the nanostructural multiphase nickel hydroxide analyzed by EDX

Elements	Nanostructural multiphase nickel hydroxide		β-$Ni(OH)_2$	
	Element (%)	Atomic (%)	Element (%)	Atomic (%)
Ni	18.64	23.46	25.35	25.53
Co	0.71	0.9	0.96	0.97
Zn	1.15	1.3	1.21	1.09
Mn	2.86	3.85		
O	15.26	70.49	19.6	72.42

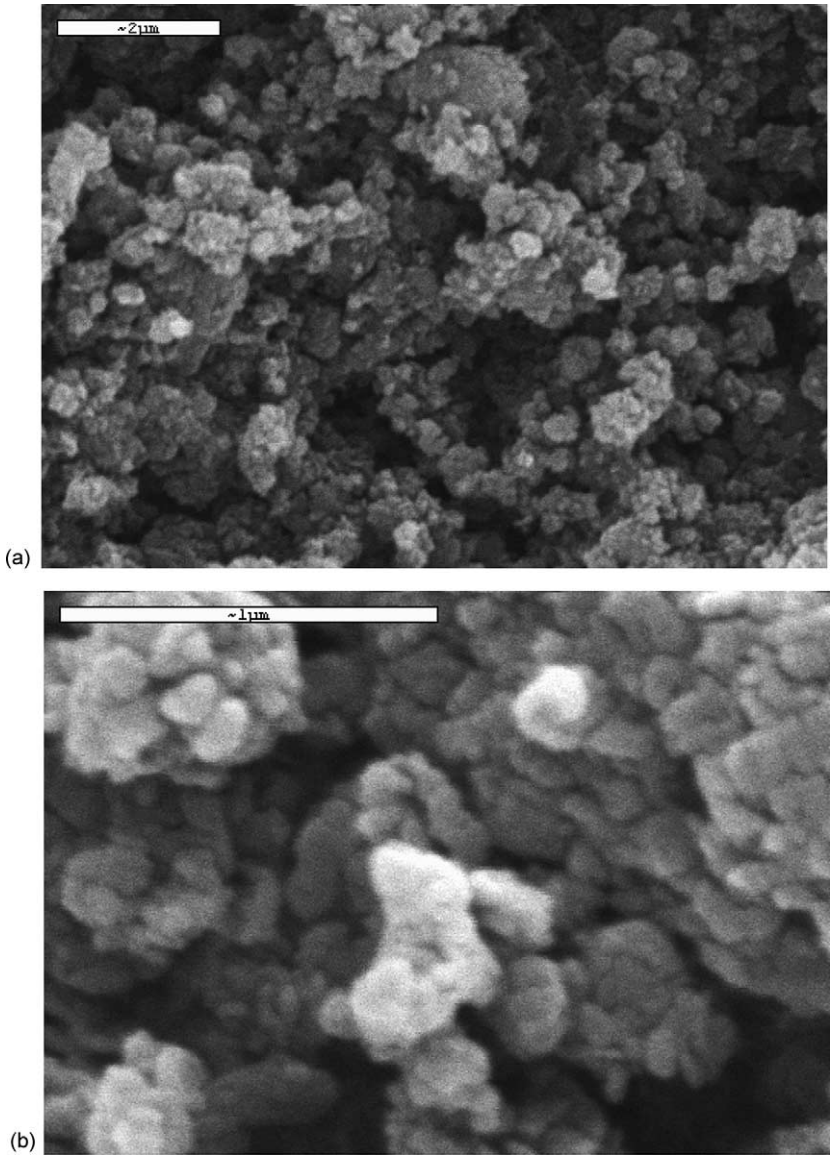

Fig. 1. SEM micrograph of the nanostructural multiphase nickel hydroxide, (a) 6000×, (b) 16,000×.

hydroxide is nearly same like that of commercial spherical nickel hydroxide and higher than that of α-$Ni(OH)_2$ reported in the literature.

The doped metal ions are most preferably Co, Zn, and Mn. Table 1 is the composition of the nanostructural multiphase nickel hydroxide determined by EDX. Chemical iodometric titration was used to determine the state of doped metal ions in nanostructural multiphase nickel hydroxide, and the results showed that a part of the cobalt introduced as Co^{2+} in the solution is spontaneously oxidized to Co^{3+}, while Mn^{2+} is spontaneously oxidized to Mn^{3+} or Mn^{4+}. Fig. 2 shows the powder X-ray diffraction pattern of the nanostructural multiphase nickel hydroxide. In the XRD patterns no diffraction pattern attributable to impurities was observed, it was assumed that they were dissolved in nickel hydroxide to form a solid solution [15]. To account for the charge imbalance created by the manganese and cobalt substitution, Audemer et al. [2] and Demourgues and Delmas [9] proposed that the presence of excess positive charge due to Co^{3+} and Mn^{3+} or Mn^{4+} ions be compensated by the insertion of anion (OH^- or CO_3^{2-}) between the slabs. This spontaneous anion insertion could give rise to an interstratified material showing a disorder in the periodicity of the (0 0 1) planes. Such a structure consists of α-$Ni(OH)_2$ (7.5 Å) and β-$Ni(OH)_2$ (4.6 Å) interconnected structural units. This explanation would be consistent with the powder X-ray diffraction patterns that show a ''peak-foot'' due to the stacking disorder, on the left if the main (0 0 1) Bragg peak. This anomaly is totally absent from the pure β-$Ni(OH)_2$ samples. It should be noted in Fig. 2a that both α-$Ni(OH)_2$ and β-$Ni(OH)_2$ peaks appear simultaneously in the diffraction patterns. The patterns were very similar to the

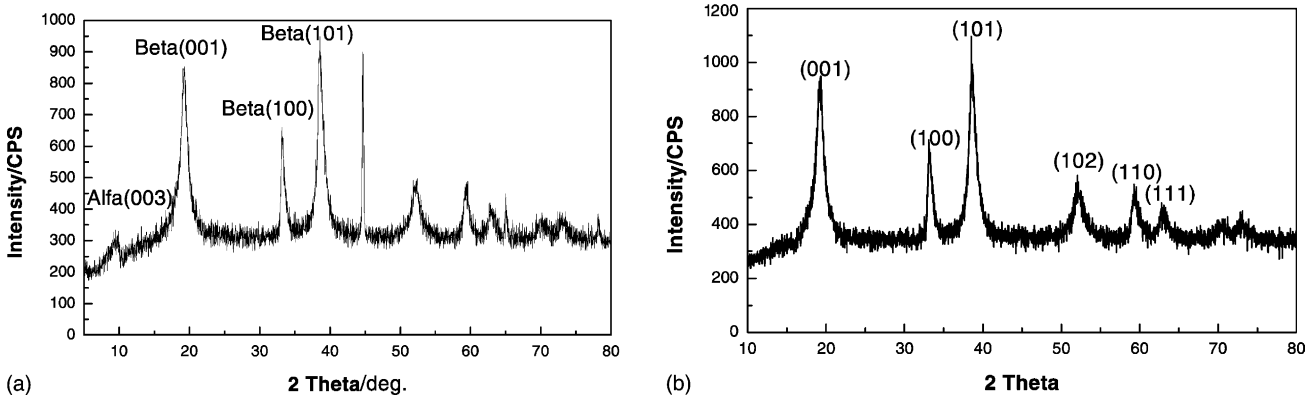

Fig. 2. X-ray diffraction patterns for (a) the nanostructural multiphase nickel hydroxide and (b) β-Ni(OH)$_2$.

theoretically generated patterns based on the interstratified structure developed by Demourgues et al. [10]. Therefore, in Fig. 2 the XRD patterns of the nanostructural multiphase nickel hydroxide has a mixed phase structure as compared to unsubstituted α-Ni(OH)$_2$ and β-Ni(OH)$_2$ reported in the literature [13,14]. They show a low angle reflection close to 6.97 Å, followed by another at around 3.96 Å. In addition, nanostructural multiphase nickel hydroxide show broad asymmetric band in the 2.2–2.6 Å, this is the typical structure of turbostratic structure.

It been also seen from Fig. 2 that the characteristic line (6.97 Å) representing α-Ni(OH)$_2$ is slightly lower than the one (7.5 Å) of pure α-Ni(OH)$_2$. The reason of this change is that due to the introduction of high valence cations, the crystal structure of α-Ni(OH)$_2$ occurred some changes. As stated above, both structures of α-Ni(OH)$_2$ and β-Ni(OH)$_2$ consist of brucite-type layers well ordered along the *c*-axis (β-Ni(OH)$_2$) or randomly stacked along the *c*-axis (α-Ni(OH)$_2$) with, for the latter, water molecules and anionic species within the Van der Waals gap resulting in a *c*-spacing of 7.5 Å. Compared to 4.8 Å for the β-Ni(OH)$_2$, pure α-Ni(OH)$_2$ is a pure divalent material and anions intercalation occurs more on account of hydroxyl ion vacancies rather than due to the exigencies of charge compensation [15]. Consequently, its bonding strength with the brucite layer is also poor. This also account for the poor stability of α-Ni(OH)$_2$ in alkali media. Introducing Mn, Co and Zn ions in the nickel hydroxide lattice, with the purpose of enhancing the intercalated anion content successfully stabilizes the α-Ni(OH)$_2$ structure under alkali media. The charge excess due to high valence cations are compensated by the insertion of carbonate between the hydroxide slabs. The anions strongly anchor the positive charged brucite layers and stabilize the structure in a variety of stressful conditions.

Usually, α-Ni(OH)$_2$ is unstable in alkaline medium and easily changed into β-Ni(OH)$_2$. Fig. 3 shows the XRD patterns of the aged samples (in 6 M KOH for 7 days). It can be seen from Fig. 3 that the sample do not show any structural change except for the characteristic peak (0 0 3) of α-Ni(OH)$_2$ slightly broadened after aged, and thus the sample is still a mixed structure of stabilized α-Ni(OH)$_2$ and β-Ni(OH)$_2$. This implies that the nanostructural multiphase nickel hydroxide will have a structural stability during charge/discharge.

Fig. 4 is the IR spectra of the nanostructural multiphase nickel hydroxide. There is a sharp peak in the region 3700–3300 cm^{-1}. This sharp peak in the OH stretching region is shown by α-Ni(OH)$_2$ or β-Ni(OH)$_2$ because of the absence of hydrogen bonding between hydroxyl groups. The peaks in the 800–1800 cm^{-1} range could be due to the presence of anions which are probably not completely eliminated during the washing stage. The band centered around 460 cm^{-1} is the Ni–O stretching mode.

Several other bands were observed but the prominent feature of the spectra is the presence of a δ-H$_2$O infrared line located at 1630 cm^{-1}. Comparing the absorption at ca. 3440 cm^{-1}and the δ_{H-O-H} bands 1630 cm^{-1}, one concludes that nanostructural multiphase nickel hydroxide is more hydrated than β-Ni(OH)$_2$, in agreement with [16], while a number of bands at 1500–1000 cm^{-1} reveal the presence of anion impurities, e.g. CO_3^{2-} [16]. The line at 1630 cm^{-1} generally ascribed to water molecules adsorbed on the surface of the particles. The surface adsorbed water molecules, which are bound by hydrogen bonds can increase further

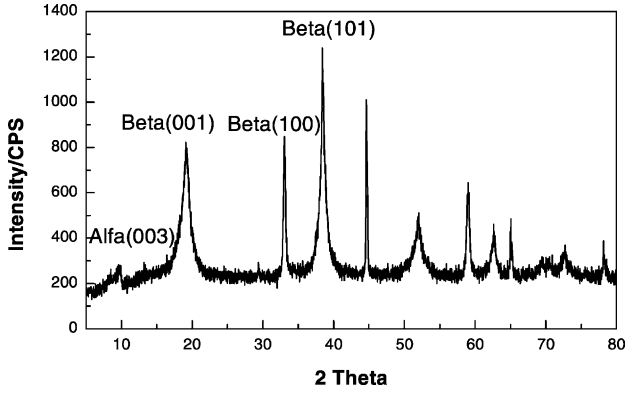

Fig. 3. X-ray diffraction patterns for aging nanostructural multiphase nickel hydroxide.

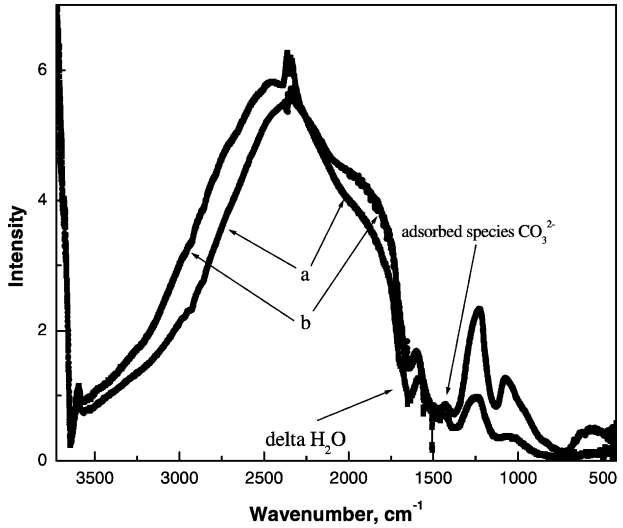

Fig. 4. IR spectra for (a) the nanostructural multiphase nickel hydroxide and (b) β-Ni(OH)$_2$.

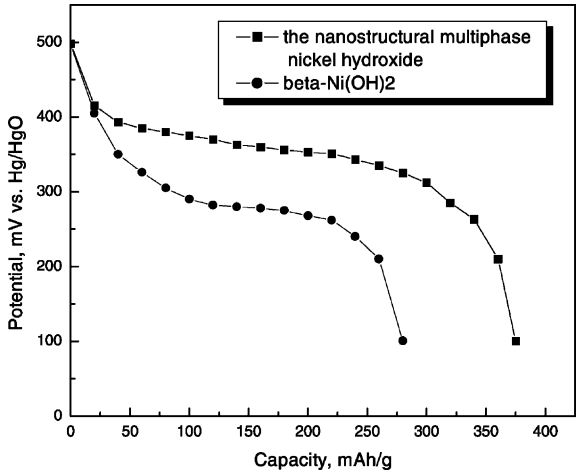

Fig. 5. Discharge curves for (a) the nanostructural multiphase nickel hydroxide electrode and (b) β-Ni(OH)$_2$ electrode at a rate of 0.2*C*.

with increasing surface area. Audemer et al. [2] found that the electrochemical performances of nickel hydroxide were not related to its spherical feature but they were related to their surface area, while the spherical morphology of the agglomerates is only useful for ensuring a high packing density during the electrode-forming process. Existence of nanosturctural particles can apparently improve the surface area of the nanostructural multiphase nickel hydroxide that results in an increasing amount of absorbed water molecules on the surface of the particles. This surface water is believed to improve the nickel hydroxide particles wettability [2], thus resulting in an enhanced proton transport within the active material during the charge/discharge process, and thereby a better utilization of the electrode material. Besides, comparing the area of the peak at 1630 cm^{-1} in Fig. 4, it can been found that the area of the nanostructural multiphase nickel hydroxide was slightly bigger than one of β-Ni(OH)$_2$. Although this cannot quantitatively been illustrated the absorbed water amount, it can qualitatively explicated that nanostructural multiphase nickel hydroxide has much more water amount than β-Ni(OH)$_2$. This indicated that due to its nanostructural multiphase, some water molecule inserted interlayer except for absorbed water molecule, and thus improving its electrochemical activity.

Fig. 5 shows the discharge curves of spherical β-Ni(OH)$_2$ electrode and the nanostructural multiphase nickel hydroxide electrode at a rate of 0.2*C*. As seen from Fig. 5, the discharging capacity of the nanostructural multiphase nickel hydroxide electrode was markedly higher than that of spherical β-Ni(OH)$_2$. The discharge capacity of the nanostructural multiphase nickel hydroxide electrode is 375 mAh/g. Apparently, this result is higher than the theoretical capacity of usual spherical β-Ni(OH)$_2$ electrode. Traditionally, the theoretical capacity of nickel hydroxide electrode was believed to be 289 mAh/g if the electrode reaction during charge/discharge process involves one-electron transfer. According to calculating result on the base of theoretical capacity, the exchange electron numbers of the nanostructural multiphase nickel hydroxide electrode during charge/discharge process were 1.3 numbers. Although this measured result is slightly lower than that calculated according to electrochemical measurement our previously reported [12], it is markedly higher than of that of spherical β-Ni(OH)$_2$. It also can be seen from Fig. 5 that the discharging potentials for the electrodes of two types had an initial fall from between 400 and 500 mV to less than 350 mV, followed by a more stable region in each curve. Below 250 mV the discharging potentials decrease rapidly. In addition, the nanostructural multiphase nickel hydroxide electrode exhibited a clearly increased discharging potential plateau region in Fig. 5. The discharge potential plateau of the nanostructural multiphase nickel hydroxide electrode is nearly higher than 100 mV than one of β-Ni(OH)$_2$ electrode.

Fig. 6 shows the 25th cyclic voltammograms of the spherical β-Ni(OH)$_2$ electrode and the nanostructural multiphase nickel hydroxide electrode at a potential scanning rate of 5 mV/s. In the range of scanning potentials employed, although those were recorded prior to oxygen evolution, anodic oxidation peaks for the electrodes revealed evident difference. For the nanostructural multiphase nickel hydroxide electrode, the anodic oxidation peak split into two peaks, one appeared in about 270 mV, and another is about 331 mV; oppositely for usual spherical β-Ni(OH)$_2$ electrode, only one anodic oxidation peak at about 330 mV was recorded. Similar voltammogram has also been observed [13], the first oxidation peak was ascribed to oxidation of α-Ni(OH)$_2$ and second oxidation peak to oxidation of β-Ni(OH)$_2$. While for reduction process of nickel oxyhydroxide, only one oxyhydroxide reduction peak for two electrodes at about 149 and 136 mV, respectively, was observed on the reverse sweep. Apparently, the reduction peak of the nanostructural multiphase nickel hydroxide electrode is

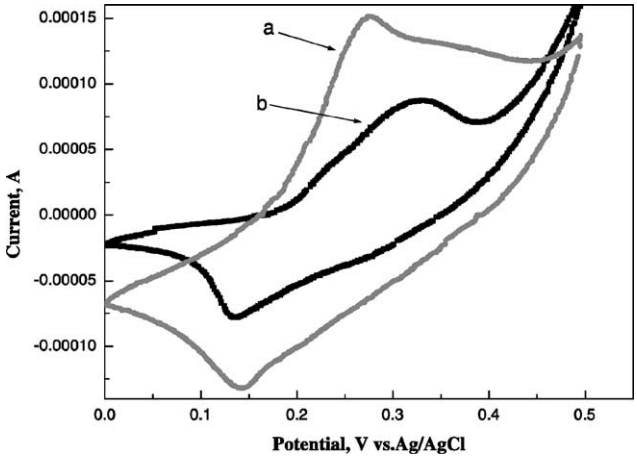

Fig. 6. Cyclic voltammograms of the nanostructural multiphase nickel hydroxide electrode and β-Ni(OH)$_2$ electrode.

higher than one β-Ni(OH)$_2$ electrode. Besides, it can be known from the peak area in Fig. 6 that the nanostructural multiphase nickel hydroxide electrode has much higher discharge capacity than β-Ni(OH)$_2$ electrode. Kim et al. [13] reported the cyclic voltammogram results of α-Ni(OH)$_2$ film which was electrochemically precipitated on the surface of a gold evaporated quartz crystal and found that the anodic scan only showed an anodic current peak at 449 mV versus Hg/HgO and the cathodic scan exhibited a cathodic current peak at 362 mV versus Hg/HgO. Similarly, Kim et al. [13] also reported the cyclic voltammogram results of β-Ni(OH)$_2$ film which was obtained by aging the cathodically precipitated α-Ni(OH)$_2$ film for 4 h in a 6 M KOH solution at 50 °C and found that the anodic scan exhibited an anodic peak at 514 mV versus Hg/HgO, which was 65 mV higher than that of α-Ni(OH)$_2$, and a serious oxygen evolution occurred at potential over 550 V versus Hg/HgO; while cathodic scan exhibited a cathodic current peak at 376 mV versus Hg/HgO. The measured results in Fig. 6 were in agreement with Kim et al. [13]. Due to doping, some modifier elements and existence of nanostructural multiphase, electrochemical performance of the sample in Fig. 6 were markedly superior to the ones of α-Ni(OH)$_2$ and β-Ni(OH)$_2$.

As shown in Fig. 6, the anodic oxidation peak of the nanostructural multiphase nickel hydroxide apparently split into two oxidation peaks of α-Ni(OH)$_2$ and β-Ni(OH)$_2$, respectively. For the nanostructural multiphase nickel hydroxide, the two anodic oxidation peaks corresponding to Ni(II) oxidation reaction shift to less positive potentials, and cathodic peak potential corresponding to nickel oxyhydroxide reduction reaction also slightly shifts to less positive compared to the characteristics of β-Ni(OH)$_2$. The cyclic voltammetric results in Fig. 6 are tabulated in Table 2. In Table 2, the difference between the anodic and cathodic peak positions, $\Delta E_{a,c}$, is taken as an estimate of the reversibility of the redox reaction. Oxygen evolution is a parasitic reaction during charge of nickel electrode. To compare the effect of the nanostructural multiphase nickel hydroxide electrode on oxygen evolution reaction, the difference between the oxidation peak potential and the oxygen evolution potential (DOP) on the return sweep required to produce 1.25×10^{-4} A of anodic current is also estimated from voltammograms [17,18].

The results in Fig. 6 and Table 1 illustrated that the nanostructural multiphase nickel hydroxide allows the electrode to charge at a significantly less positive potential (273 and 331 mV) instead of 330 mV. In addition, the charge process appear to occur more reversibly ($\Delta E_{a,c}$ is 124 and 182 mV instead of 194 mV). Moreover, oxygen evolution overpotential shift to a more positive value ((DOP is 225 and 167 mV instead of 146 mV). Thus, these results showed that the nanostructural multiphase nickel hydroxide electrode allows the charge process to occur more easily and more reversibly, indicating that much more active material can be utilized during charge. Besides, due to the increase in the oxygen evolution overpotential and the decrease of the oxidation peak potential of Ni(II), the charge efficiency of the electrode could markedly be improved, this implies that the electrode will has a greater discharge capacity.

When the nanostructural multiphase nickel hydroxide electrode was carried out cyclic voltammogram measurements, an interesting phenomenon occur, that is, there was not the oxidation peak of α-Ni(OH)$_2$ at starting experiment, however with continuing cyclic voltammograms the anodic oxidation peak split into two current peak, that is, the oxidation peak of α-Ni(OH)$_2$ appeared gradually and the intensity of peak increased gradually. After about 15 cyclic voltammograms, the oxidation peak of α-Ni(OH)$_2$ is higher than one of β-Ni(OH)$_2$. Fig. 7 shows a series of recorded voltammetric scans. As seen in Fig. 7, only one sharp oxidation peak located at 0.378 V in the fifth oxidation–reduction cycle was observed. With increasing cycles the oxidation peak of α-Ni(OH)$_2$ occurred gradually. Bernard

Table 2
The comparison of parameters of cyclic voltammograms

Electrode	E_{pa1} (V) vs. Ag/AgCl	E_{pa2} (V) vs. Ag/AgCl	E_{pc} (V) vs. Ag/AgCl	$\Delta E_{a,c1}$ (V)	$\Delta E_{a,c2}$ (V)	DOP1 (V)	DOP2 (V)
Nanostructural multiphase nickel hydroxide	0.273	0.331	0.149	0.124	0.182	0.225	0.165
β-Ni(OH)$_2$	0.330		0.136	0.194		0.146	

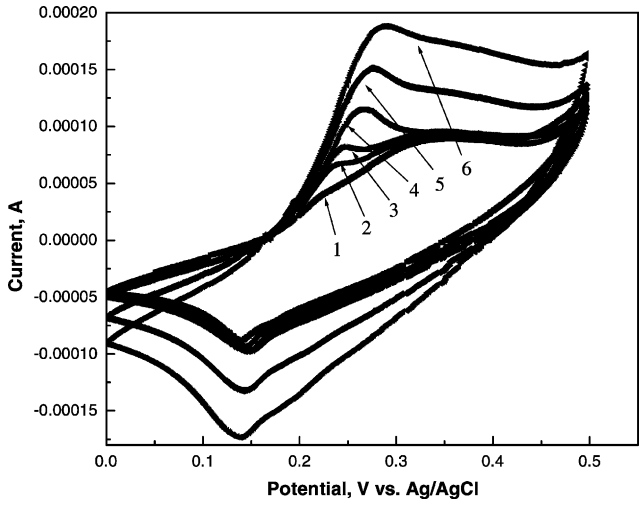

Fig. 7. Cyclic voltammograms of the nanostructural multiphase nickel hydroxide electrode at different cycles.

et al. [19] carried successive cyclic voltammogram for α-$Ni(OH)_2$ electrode and found that the potential of the oxidation peak shifted toward more anodic values, thus they believed that the changes of the electrochemical properties were associated with a phase transformation of the precursor α-$Ni(OH)_2$ into a β-$Ni(OH)_2$. Kostecki and Mclarnon [15] studied pure nickel hydroxide and observed similar phenomena for the cyclic voltammogram of the freshly prepared α-$Ni(OH)_2$ electrode. It can be seen from Fig. 7 that the positions of the oxidation and reduction peak of the nanostructural multiphase nickel hydroxide did not nearly change with increasing cycles and the intensity of oxidation peak of α-$Ni(OH)_2$ increased gradually. Therefore, it can be believed that the nanostructural multiphase nickel hydroxide electrode had a stable cycle and did not occur the change of structure during charge/discharge process.

Kim et al. [13] studied α-$Ni(OH)_2$ electrode with cyclic voltammetric method and found similar phenomena for aging process of α-$Ni(OH)_2$, they believed that intermediates phase were formed during aging of α-$Ni(OH)_2$. Analysis of the XRD patterns and the cyclic voltammograms as shown in Figs. 2, 3, 6 and 7 suggests that the nanostructural multiphase nickel hydroxide was not same like both α-$Ni(OH)_2$ and β-$Ni(OH)_2$, it was similar to intermediate phase compound reported by Kim et al. [13]. The intermediate phase compound had the interstratified structure and was consisted of two components, one part is similar to α-$Ni(OH)_2$ with a long intersheet distance; and the other similar to β-$Ni(OH)_2$ with a short intersheet distance. However, since high valence cations partly substituted the nickel atom in nickel hydroxide lattice, the intersheet distance similar to α-$Ni(OH)_2$ had some slight change.

According to the above analysis and discussion, it can be concluded that the nanostructural multiphase nickel hydroxide has a mixed phase structure, it has not only an excellent electrochemical performance, but also a long term structure stability during charge/discharge process.

4. Conclusion

(1) A mixed phase structure compound, which was similar to intermediate phase compound of α-$Ni(OH)_2$ and β-$Ni(OH)_2$, has been synthesized through doping some modifier elements and chemical co-precipitation. The compound consisted of a series of nanostructural particles. XRD measurements showed that the compound had a mixed phase of α-$Ni(OH)_2$ and β-$Ni(OH)_2$, but the intersheet distance which was similar to α-$Ni(OH)_2$ slightly became short.

(2) Since there was a mixed phase structure, the anodic oxidation peak of the nanostructural multiphase nickel hydroxide electrode on the cyclic voltammogram split into two peaks, that is, one is the oxidation peak of α-$Ni(OH)_2$, and another the oxidation peak of β-$Ni(OH)_2$; while only one reduction peak was observed in the reverse scan.

(3) The nanostructural multiphase nickel hydroxide electrode exhibits excellent electrochemical performance, which was markedly superior to the ones of α-$Ni(OH)_2$ and β-$Ni(OH)_2$, such as allowing the charge process to occur more easily and more reversibly, and oxygen evolution overpotential shift to a more positive value.

(4) The nanostructural multiphase nickel hydroxide electrode has a long term structural stability during charge/discharge process. The tap-density reach 1.7–1.9 g/cm^3, the discharge capacity of the electrode can reach 375 mAh/g. Therefore, it can be believed that the nanostructural multiphase nickel hydroxide is a promising positive active material for alkaline recharge material.

Acknowledgements

The authors appreciate the assistance of Mr. Maunel Plaues in Electron Microscope Central, Polytechnic University of Valencia. This project is supported by the Excellent Youth Fund of Hunan Province Educational Committee, China, and Universidad Politecnica de Valencia, Spain.

References

[1] M. Oshitani, H. Yufu, K. Takashima, S. Tsuju, J. Electrochem. Soc. 136 (1989) 1590.
[2] A. Audemer, A. Delahaye, R. Farhi, N. Sac-Epee, J.-M. Tarascon, J. Electrochem. Soc. 144 (1997) 2614.
[3] P. Genin, A. Delahaye-Vidal, F. Portemer, K. Tekaia-Elhsissen, M.F. Iglarz, Eur. J. Solid State Inorg. Chem. 28 (1991) 505.
[4] R. Barnard, C.F. Randell, F.L. Tye, J. Appl. Electrochem. 10 (1980) 109.
[5] P.V. Kamath, M. Dixit, L. Indira, A.K. Shukla, V.G. Lumar, N. Munichandraiah, J. Electrochem. Soc. 141 (1994) 2956.
[6] M. Dixit, R.S. Jayashree, P.V. Kamath, A.K. Shukla, V.G. Kumar, N. Munichandraiah, Electrochem. Solid State Lett. 2 (1999) 170.
[7] C. Faure, C. Delmas, M. Fouassier, J. Power Sources 35 (1991) 279.

[8] B.B. Ezhov, O.G. Malandin, J. Electrochem. Soc. 138 (1991) 885.
[9] L.G. Demourgues, C. Delmas, J. Electrochem. Soc. 143 (1996) 561.
[10] L.G. Demourgues, C. Denage, C. Delmas, J. Power Sources 52 (1994) 269.
[11] J. Dai, S.F.Y. Li, J. Power Sources 89 (1) (2000) 40.
[12] X. Wang, P.V. Parkhutik, unpublished manuscript.
[13] M.-S. Kim, T.-S. Hwang, K.-B. Kim, J. Electrochem. Soc. 144 (1997) 1537.
[14] P. Oliva, J. Leonardi, J.F. Laurent, C. Delmas, J. Barconnier, M. Figlarz, F. Fievet, A. De Guibert, J. Power Sources 8 (1992) 229.
[15] R. Kostecki, F. Mclarnon, J. Electrochem. Soc. 144 (1997) 485.
[16] A.A. Kamnev, A.A. Smekhnov, Fresenius J. Anal. Chem. 355 (1996) 710.
[17] D.A. Corrigan, R.M. Bendert, J. Electrochem. Soc. 136 (1989) 723.
[18] X. Wang, J. Yan, Y. Zhang, J. Power Sources 72 (1997) 221.
[19] M.C. Bernard, P. Bernard, M. Keddam, S. Senyarich, H. Takenouti, Electrochim. Acta 41 (1996) 91.